



## Research article

High resolution UPLC-PDA-QTOF-ESI-MS/MS analysis of the flavonoid-rich fraction of *Lasianthera africana* leaves, and *in vivo* evaluation of its renal and cardiac function effectsDaniel Emmanuel Ekpo<sup>a,\*</sup>, Parker Elijah Joshua<sup>a,\*\*</sup>, Joyce Oloaigbe Ogidigo<sup>a,b</sup>, Okwesilieze Fred Chiletugo Nwodo<sup>a,c</sup><sup>a</sup> Department of Biochemistry, Faculty of Biological Sciences, University of Nigeria, 410001, Nsukka, Enugu State, Nigeria<sup>b</sup> Bioresources Development Centre, National Biotechnology Development Agency (NABDA), Federal Capital Territory, Abuja, Nigeria<sup>c</sup> Department of Biochemistry, Faculty of Medical, Pharmaceutical and Health Sciences, University of Mkar, Mkar, Benue State, Nigeria

## ARTICLE INFO

## Keywords:

Antioxidants  
 Cardiac enzymes  
 Carbon tetrachloride  
 Flavonoid-rich fraction  
 Isolation and characterization  
*Lasianthera africana* P. Beauv.  
 Oxidative stress  
 Polyphenolic phytochemicals  
 Reactive oxygen species  
 Renal function  
 UPLC-PDA-QTOF-ESI-MS/MS  
 Biological sciences  
 Ethnopharmacology  
 Pharmaceutical science  
 Natural product  
 Toxicology

## ABSTRACT

*Lasianthera africana* P. Beauv. (Icacinaeae) is a traditional Nigerian medicinal plant used for treatment of ulcers, diarrhea, parasitic infections and diabetes. This study was aimed at characterizing the bioactive principles extractable from the flavonoid-rich fraction of *L. africana* leaves (LAFRF), and to evaluate its effects on renal and cardiac functions. Isolation, and purification of the LAFRF was achieved using standard methods. The *in vitro* antioxidant activity was evaluated on DPPH\* and ferric reducing antioxidant potential (FRAP). The total flavonoids ( $281.05 \pm 7.44$  mg QE/g), were identified, structurally characterized and quantified using high resolution ultra-performance liquid chromatography, in tandem with quadrupole-time-of-flight electrospray ionization mass spectrometer (UPLC-PDA-QTOF-ESI-MS/MS). Fifty Wistar rats of both sexes (110–130 g), were distributed into 10 groups (n = 5). Groups 1 and 2 served as the normal and CCl<sub>4</sub> controls respectively. Groups 3A-6B constituted the preventive and curative studies. The effects of the LAFRF at 3, 10, and 30 mg/kg body weight on urea and creatinine concentrations, lactate dehydrogenase (LDH), and creatine kinase (CK) activities of CCl<sub>4</sub>-intoxicated rats were assessed. The LAFRF displayed remarkable *in vitro* antioxidant property by scavenging the DPPH\*, with an IC<sub>50</sub> of  $5.40 \pm 0.00$  µg/ml which is more potent than the scavenging activity of the ascorbic acid (IC<sub>50</sub> of  $7.18 \pm 0.00$  µg/ml), and also effectively reduced Fe<sup>3+</sup> to Fe<sup>2+</sup> when compared to gallic acid. The UPLC-PDA-QTOF-ESI-MS/MS fingerprint of the LAFRF indicated presence of quercetin (758983.6 mg/kg), rutin (17540.4 mg/kg), luteolin (126524.3 mg/kg), isorhamnetin (197949.0 mg/kg), and other non-phenolic compounds. The LAFRF significantly (p < 0.05) improved renal function, and normalized cardiac enzyme activities *in vivo*. The ability of the LAFRF to scavenge the DPPH and Fe<sup>3+</sup> radicals, improve renal and cardiac functions following CCl<sub>4</sub> intoxication shows its potential in the development of alternative therapy for combating oxidative stress-related complications.

## 1. Introduction

Medicinal plants and their extracts contain many phytochemical compounds such as flavonoids and other phenolic compounds which have therapeutic effects through their antioxidant properties, and effects on oxidative stress. These active ingredients have been the source of medicines over the years and may still be the leads for discovery of new drugs (Newman, 2008). Oxidative stress is a result of redox disequilibrium in which the pro-oxidant/antioxidant balance is shifted in favor of

the pro-oxidants (Videla, 2009). This condition can lead to damage of lipids, proteins, carbohydrates, and nucleic acids (Glantzounis et al., 2005). Excessive production of reactive oxygen species (ROS) induces oxidative stress which can result in lipid peroxidation and subsequent damage to cell membrane architecture, with a consequent alteration in metabolic processes (Shah et al., 2015). ROS also play a crucial role in the pathogenesis of different human diseases including liver, heart, lung, and kidney disorders (Singh et al., 2008). A well maintained pro-oxidant/antioxidant balance exists between the production of free

\* Corresponding author.

\*\* Corresponding author.

E-mail addresses: [ekpodaniele@gmail.com](mailto:ekpodaniele@gmail.com), [daniel.ekpo.pg67714@unn.edu.ng](mailto:daniel.ekpo.pg67714@unn.edu.ng) (D.E. Ekpo), [parker.joshua@unn.edu.ng](mailto:parker.joshua@unn.edu.ng) (P.E. Joshua).

radicals and their rates of removal by various antioxidant defense mechanisms in a healthy individual (Rekha et al., 2012).

Antioxidants are compounds that inhibit oxidation; a chemical reaction which produces free radicals, leading to chain reactions that may damage cells of organisms. Principally, antioxidants act by interrupting, averting or eliminating oxidative damage to a target molecule. Antioxidants such as flavonoids are excellent singlet and triplet oxygen quenchers, free radical scavengers, peroxide decomposers, enzyme inhibitors, and synergists (Manach et al., 1998). They are polyphenolic antioxidant phytochemicals consisting of flavones, flavanone, flavanols, flavonols and flavanonols that make up a large group of secondary metabolites in plants (Chua et al., 2011). They are known to act by quenching free radical elements, chelating key metal, suppressing the enzymes associated with free radical generation and stimulation of internal antioxidant enzymes (Nema et al., 2009). Even at relatively low concentrations, flavonoids still maintain a remarkable number of biological activities and pharmacological effects (Procházková et al., 2011).

The exposure to environmental pollutants and chemical toxicants results in the production of toxic free radicals within biological systems, causing lipid peroxidation, loss of membrane integrity and ultimately, damage to tissues and cells of organisms. This exposure can come from the air, drinking water, foodstuffs, soil, and some industrial sites where these chemicals are used, or where industrial contamination had occurred. Carbon tetrachloride (CCl<sub>4</sub>) is a known chemical toxin whose bio-activation within the living systems produces highly reactive trichloromethyl radical (CCl<sub>3</sub>\*), and trichloromethyl peroxy radical (CClOO<sub>3</sub>\*). These radicals cause damage to macromolecules such as lipids, proteins and deoxyribonucleic acids (DNA), affecting key organs such as the liver, kidneys, and heart. *Lasianthera africana*, P. Beauv (icacinaceae) (Figure 1) is an edible and medicinal plant, locally known as “Editan” in Ibibio and Annang tribes of Southern Nigeria, and is traditionally used for the treatment of diarrhea, dysentery, stomach troubles, parasitic infections, ulcers and diabetes (Andy et al., 2008). The leaves of the plant have been reported to contain different phytochemicals possessing antimalarial (Okokon et al., 2007), antiulcerogenic (Okokon et al., 2009), antimicrobial (Andy et al., 2008), antidiabetic (Ekanem et al., 2016), hypoglycaemic (Essien and Effiong, 2017), and antioxidant activities (Atiko et al., 2016). Flavonoids and phenols are excellent scavengers of free radicals and their compositions in plants can be easily characterized by high resolution ultra-performance liquid chromatography in tandem with a quadrupole-time-of-flight electrospray ionization mass spectrometer (UPLC-PDA-QTOF-ESI-MS/MS). Hence, the aim of this study was to characterize the bioactive principles, extractable from the flavonoid-rich fraction of *L. africana* leaves (LAFRF), and to evaluate its effects on indices of renal and cardiac functions in adult Wistar rodent model.

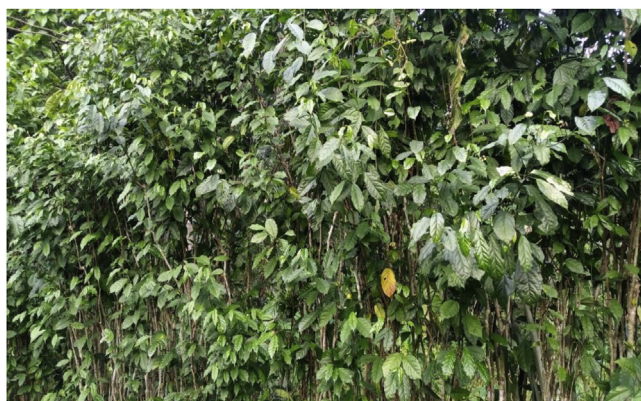


Figure 1. *Lasianthera africana* shrub.

## 2. Materials and methods

### 2.1. Materials

#### 2.1.1. Procurement, identification and authentication

Fresh leaves of *L. africana* P. Beauv (Figure 1), were collected from Ukana Akpautong, Ikot Akpantia village in Essien Udim Local Government Area of Akwa Ibom State, Nigeria, in October 2018. The leaf sample was identified and authenticated by Mr. Felix Nwafor, a plant taxonomy and Bioinformatics specialist. A voucher specimen (PCG/UNN/0315) was deposited at the Herbarium of the Department of Pharmacognosy and Environmental Medicine, University of Nigeria, Nsukka, Nigeria. The identity and authenticity of the plant was also confirmed with the one deposited in the databases of <http://www.theplantlist.org/>, and <http://www.ipni.org/>.

#### 2.1.2. Study rodents

Nine weeks old and healthy adult Wistar rats of both sexes, were purchased from the Animal House of the Department of Zoology and Environmental Biology, University of Nigeria, Nsukka, and were kept in well ventilated laboratory cages in the Animal House of the Department of Biochemistry, University of Nigeria, Nsukka. They were acclimatized to the laboratory environment for a period of seven days under standard environmental conditions, with a 12 h light/dark cycle prior to experimentation. The animals were maintained on standard animal feed and drinking water *ad libitum*. They received humane care throughout the duration of the animal study, in line with the regulations and ethical approval of the Ethics and Biosafety Committee of the Faculty of Biological Sciences, University of Nigeria, Reference No: UNN/FBS/EC/2019/1007, and in accordance with the National and International Ethical Recommendations for Care and Use of Laboratory Animals (National Academy of Sciences [NAS], 2011).

#### 2.1.3. Chemicals and reagents

All chemicals and reagents used for this study were of analytical grade. Quercetin (purity >98%), gallic acid (purity >98%), and L-ascorbic acid (purity >99%), 1, 1-diphenyl-2-picrylhydrazyl (purity ≥90%), UHPLC grade acetonitrile (purity ≥99.93), formic acid, and Dowex® ion exchange resin, 50WX8 hydrogen form, were purchased from Sigma-Aldrich, Inc., (St Louis, USA). Sodium trioxocarbonate (VI), ferric trichloride hexahydrate, iron (II) tetraoxosulphate (VI), and potassium bromide were purchased from Qualikems Laboratories (India). Absolute ethanol (purity ≥95%), methanol (≥99.8%), ethyl acetate (≥99.5%), hydrochloric acid, were purchased from (BDH Chemicals Ltd., (Poole, England). The water used for all analysis was glass distilled.

### 2.2. Methods

#### 2.2.1. Plant preparation and processing

The harvested leaves of *L. africana* were carefully separated from the stem, freed from sand and debris, and air-dried to a constant weight. The dried plant leaves were pulverized into powdered form and used for crude extraction.

#### 2.2.2. Extraction of bioactive components

The crude plant extraction in this study followed the protocol of Kumar et al. (2014), with some modifications. Briefly, 3200 g of the dried and powdered plant sample was extracted with (80%) methanol in distilled water using cold maceration method for 72 h. The extract was filtered using a muslin cloth, with further filtration achieved using Whatman No.1 filter paper. The filtrate obtained was centrifuged at 6000 rpm for 10 min to remove fine suspended particles. The solvent was then removed at reduced pressure to obtain the methanol extract of *L. africana* leaves subsequently referred to as the MELA (Figure 2A).

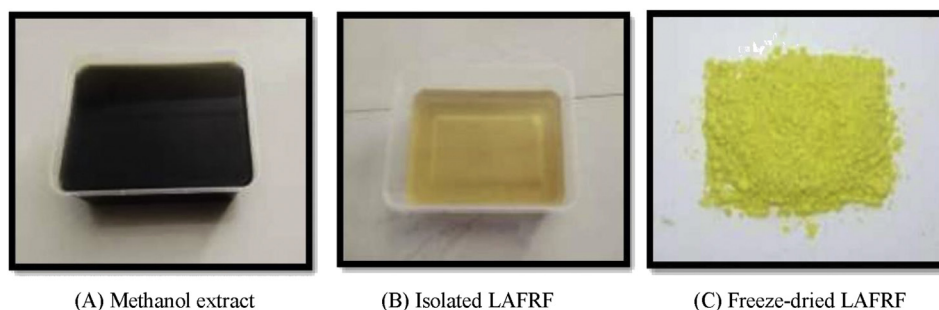


Figure 2. Methanol extract and flavonoid-rich fractions of *L. africana* leaves.

### 2.2.3. Isolation of the LAFRF

The MELA was suspended in distilled water and partitioned in ethyl acetate to obtain the ethyl acetate fraction (EAF). The EAF was again suspended in distilled water for subsequent purification by column chromatography using ion exchange resin. Resin activation and flavonoid purification from the crude plant extract (MELA) was previously reported by Omotuyi et al. (2018). The cationic exchanger, Dowex® 50WX8 hydrogen form (100–200 mesh, 100 g) was activated by overnight treatment with 2 bed volumes (BV) of distilled ethanol followed by rinsing with 5 BV of distilled water at room temperature. The activated resin was loaded on a glass column. The column was washed thoroughly with distilled and deionized water to elute sugars and unbound impurities. Bound flavonoids were eluted using 95% ethanol: 5% HCl (1% v/v) (Figure 2B). Eluted samples were pooled, freeze-dried, and subsequently referred to as the flavonoid-rich fraction of *L. africana* leaves (LAFRF) (Figure 2C).

### 2.2.4. Determination of total flavonoid concentration

The total flavonoid concentration (TFC) of the LAFRF, and the MELA was determined by the method of Zhishen et al. (1999). The test is based on the principle that aluminum ( $\text{Al}^{3+}$ ) reacts with hydroxyl groups of flavonoids forming a stable flavonoid- $\text{Al}^{3+}$  complex which produces an instant golden-yellowish coloration whose intensity is proportional to the concentration of flavonoids in the sample. Quercetin was used as the standard flavonoid for this experiment. Different concentrations (80, 40, 20, 10 and 5  $\mu\text{g}/\text{ml}$ ) of the standard and the sample were added to 3 ml methanol, 0.2 ml of 10% aluminum chloride and 0.2 ml of 1M potassium acetate. Thereafter, 5.6 ml of distilled water was added to all the tubes and the mixture was incubated at room temperature for 30 min. The absorbance of the sample was read against the reagent blank at 420 nm. The TFC of the samples were determined from the calibration plot of quercetin ( $y = 0.0054x$ ,  $R^2 = 0.9631$ ) (Figure A.1), and the results were expressed as milligram of quercetin equivalent per gram of dried plant sample (mg QE/g).

### 2.2.5. In vitro evaluation of antioxidant activity

**2.2.5.1. DPPH radical scavenging activity.** The scavenging activity of 1, 1-diphenyl-2-picrylhydrazyl radical (DPPH<sup>\*</sup>) by the LAFRF was determined according to the method of Gyamfi et al. (1999). The reaction is based on the reduction and de-colorization of the purple chromogen radical (DPPH<sup>\*</sup>) by antioxidants or reducing compounds, to the corresponding pale yellow hydrazine. The degree of color change depends on hydrogen atom donating ability of the antioxidants, and is characterized by an absorption band in methanol solution centered at about 517 nm. A decrease in absorbance of the reaction mixture indicates an increase in the radical scavenging activity. An aliquot (1 ml) of the sample or standard at different concentrations (5, 10, 20, 40, 80 and 160  $\mu\text{g}/\text{ml}$ ) in 80% methanol was mixed with 0.5 ml of 0.076 mM DPPH in methanol. The mixture was vortexed thoroughly and allowed to stand in a dark cupboard for 30 min at room temperature. Thereafter, the absorbance of the samples ( $A_s$ ) was read at 517 nm against the blank. The negative

control ( $A_0$ ) was 0.076 mM DPPH in methanol. *L*-ascorbic acid was used as the standard while 80% methanol solution was used as the blank. All measurements were carried out in triplicates. The DPPH radical scavenging activity of the sample and standard were determined as percentage (%) inhibition using the equation below:

$$\% \text{ inhibition of DPPH radical} = \frac{(A_0 - A_s)}{A_0} \times 100$$

The  $\text{IC}_{50}$  was obtained using a plot of % inhibition against different concentrations of the sample, and this represents the concentration of the sample which caused 50% inhibition of the DPPH radical, or the concentration at which 50% of the radical is scavenged.

**2.2.5.2. Ferric reducing antioxidant potential.** The ferric reducing antioxidant potential (FRAP) of the LAFRF was determined by the method of Benzie and Strain (1996). The assay is based on reduction of ferric ions ( $\text{Fe}^{3+}$ ) to ferrous ions ( $\text{Fe}^{2+}$ ) by antioxidants in acidic medium. Different concentrations of the sample and standard were mixed with 1.0 ml of 0.2 M sodium phosphate buffer (pH 6.6), and 1.0 ml of 10 mg/l potassium ferricyanide (0.1% w/v) solution in triplicate set of test tubes. The mixtures were then incubated in a water bath at 50 °C for 20 min, after which 1.0 ml of 10% trichloroacetic acid solution was added. An aliquot of 2.0 ml of the mixture was then combined with 2.0 ml of distilled water, and 400  $\mu\text{l}$  of 0.1%  $\text{FeCl}_3 \cdot 6\text{H}_2\text{O}$ . The mixture was allowed to stand for another 10 min at room temperature. The absorbance of the reaction mixture was read at 700 nm against the blank. The procedure was repeated for different concentrations of iron (II) sulphate ( $\text{Fe}^{2+}$ ). With the absorbance data obtained, a calibration curve of sample absorbances were plotted against the different concentrations to obtain the equation of the plot,  $y = 0.0008x + 0.0597$ , with a strong positive correlation coefficient of 0.9672. The FRAP of the LAFRF was extrapolated from the equation of the plot, and the results were expressed as  $\mu\text{Mol. Fe}^{2+}/\text{g}$  of dried plant sample. An increase in absorbance with respect to concentration indicates a higher reducing potential.

### 2.2.6. Molecular identification and characterization of the LAFRF total flavonoids

**2.2.6.1. Fourier transform infrared spectroscopy.** The potassium bromide (KBr) method for solid sample analysis was used for the Fourier transform infrared spectroscopy (FTIR) analysis of the LAFRF. A Shimadzu FTIR, Model IR-Affinity-1, Made in Japan instrument was used to identify the functional groups and characteristic chemical bonds (flavonoid specific) present in the LAFRF. A known sample mass of 0.4 g KBr was weighed and pulverized to the powdered form. Thereafter, 0.001 g of the freeze-dried LAFRF was mixed with the powdered KBr, and molded into a disc. The disc was inserted into the sample compartment of the instrument. Upon contact with infrared light, the sample absorbs at different frequencies which corresponds to the chemical bonds of the carbon atoms and functional groups present. The spectrum was collected at frequency region of  $500 \text{ cm}^{-1}$  to  $4000 \text{ cm}^{-1}$ .

**2.2.6.2. High resolution UPLC-PDA-QTOF-ESI-MS/MS.** Qualitative and quantitative high resolution UPLC-PDA-QTOF-ESI-MS/MS analysis of the LAFRF was carried out using the method of Stander et al. (2017). The freeze-dried sample was treated with equal volume of the extraction solvent (acetonitrile, 50% methanol in 0.1 % formic acid), with ultra-sonication and shaking overnight. An aliquot of 2 ml of the extracted sample was withdrawn and centrifuged at 14,000 rpm before being transferred into a glass vial for analysis.

A Waters Acquity ultra-performance liquid chromatograph (UPLC) in tandem with a Waters Synapt G2 Quadrupole time-of-flight (Q-TOF) mass spectrometer (MS) (Waters, Milford, MA, USA) was used for high-resolution UPLC-PDA-QTOF-ESI-MS/MS analysis. Electrospray ionization was used in the negative mode with a cone voltage of 15 V, desolvation temperature of 275 °C and desolvation gas at 650 L/h. The rest of the MS settings were optimized for best resolution and sensitivity. The mass spectra data were acquired by scanning from 150 m/z to 1500 m/z in high resolution mode as well as in MS<sup>E</sup> mode. In the MS<sup>E</sup> mode two channels of MS data were acquired, one at a low collision energy 4 V (MS<sup>1</sup>) and the second using a collision energy ramp (40–100 V) (MS<sup>2</sup>) to obtain the fragmentation patterns. Leucine enkephalin was used as the reference mass for accurate mass determination and the instrument was calibrated with sodium formate. Sample separation was achieved on a Waters HSS T3, 2.1 × 100 mm, 1.7 μm column (C18) at 50 °C. An aliquot of 3 μl of the sample volume was used and the mobile phase consisted of 0.1% formic acid (solvent A) and acetonitrile containing 0.1% formic acid (solvent B). The gradient began at 100% solvent A for 1 min and changed to 28% solvent B over 22 min in a linear way, and then moved up to 40% solvent B over 40 min. A wash step of 1.5 min at 100% solvent B was observed, followed by re-equilibration to initial conditions for 4 min. The flow rate was maintained at 0.3 ml/min with column temperature kept at 55 °C. Ion mobility data was retrieved using the same UPLC gradient and column, with IMS wave velocity set at 332 m/s, and wave height at 20.2 V.

### 2.2.7. *In vivo* bioactivity study

**2.2.7.1. Induction of oxidative damage.** CCl<sub>4</sub> in its concentrated form was diluted in olive oil in the ratio of 1:1 v/v prior to administration in order to neutralize its cytotoxicity level. Oxidative damage was induced in rats at a daily dose of 1.0 ml/kg body weight for 48 h.

**2.2.7.2. Experimental design.** Fifty (50) healthy adult Wistar rats of both sexes (110–130 g), were carefully selected and included in the study. They were randomly distributed into 10 experimental groups of 5 rats each as shown below:

Group 1: Normal control (distilled water)

Group 2: CCl<sub>4</sub> control (CCl<sub>4</sub> + distilled water)

#### Preventive study

Group 3A: 3 mg/kg b.w of the LAFRF + CCl<sub>4</sub>

Group 4A: 10 mg/kg b.w of the LAFRF + CCl<sub>4</sub>

Group 5A: 30 mg/kg b.w of the LAFRF + CCl<sub>4</sub>

Group 6A: 100 mg/kg b.w L-ascorbic acid + CCl<sub>4</sub>

#### Curative study

Group 3B: CCl<sub>4</sub> + 3 mg/kg b.w of the LAFRF

Group 4B: CCl<sub>4</sub> + 10 mg/kg b.w of the LAFRF

Group 5B: CCl<sub>4</sub> + 30 mg/kg b.w of the LAFRF

Group 6B: CCl<sub>4</sub> + 100 mg/kg b.w. L-ascorbic acid

**2.2.7.3. Experimental protocol.** In the protective study, the LAFRF was administered from day 1–10, and then injected with a double dose of CCl<sub>4</sub> via intra-peritoneal route on day 11 and 12, with the last dose given 14–16 h before sacrificing, following an overnight fast. In the curative study, CCl<sub>4</sub> was injected on day 1 and 2 via intra-peritoneal route, and the LAFRF was administered from day 3–12. On the day 13, the animals were sacrificed following an overnight fast. Fresh blood samples were

collected via cardiac puncture into sterile plain sample tubes. The samples were centrifuged at 3000 rpm for 15 min. After which the serum was carefully collected into sterile tubes and used for biochemical analysis. The heart tissues were collected and homogenized in phosphate buffer (pH 7.0). The homogenates were centrifuged at 3000 rpm for 10 min and stored in the freezer for cardiac enzyme assays.

**2.2.7.4. Biochemical analyses.** Kidney function was assessed by measuring the concentrations of urea and creatinine using the method of Bartels and Bohmer (1972) as outlined in the Randox diagnostic test kits. Serum electrolyte concentrations were determined using standard Teco diagnostic test kits. Sodium ion (Na<sup>+</sup>) concentration was determined by the method of Trinder (1951). Potassium ion (K<sup>+</sup>) concentration was determined by the method of Teri and Sesin (1958), while chloride ion (Cl<sup>-</sup>) concentration was determined using the method of Skeggs and Hochstrasser (1964). Lactate dehydrogenase (LDH) and creatine kinase (CK) activities in serum and heart tissues were assayed according to the procedures outlined in their respective Randox assay diagnostic test kits.

### 2.3. Statistical analysis

The data obtained from the *in vivo* study were analyzed using IBM Statistical Product and Service Solutions (SPSS) software, version 23. Graphpad Prism software, version 7.04 was used for analysis of data obtained from the *in vitro* antioxidant study. Significant differences in the means were established by the one-way analysis of variance (ANOVA), followed by the *post hoc* multiple comparison, and the Duncan's homogenous subset. The results were expressed as mean ± standard deviation of replicate measurements. Mean values with  $p < 0.05$  were considered statistically significant.

## 3. Results and discussion

### 3.1. Percentage yield

The extraction of 3200 g of the powdered *L. africana* leaves using methanol gave rise to 171.20 g (5.36%) of the dark green methanol extract (MELA). Partitioning of 150 g of the MELA in ethyl acetate, and subsequent purification by ion exchange chromatography gave rise to 2.853 g of the golden yellowish LAFRF which constitute 11.41% of the ethyl acetate fraction used. Different factors such as; the properties of the extraction solvent (e.g. the type and percentage of solvent used for extraction, and the solvent-to-solid ratio), the particle size of the plant materials, the nature of the leaves, leaf conditions, time of harvesting, acidification percentage, drying temperature, storage conditions, the

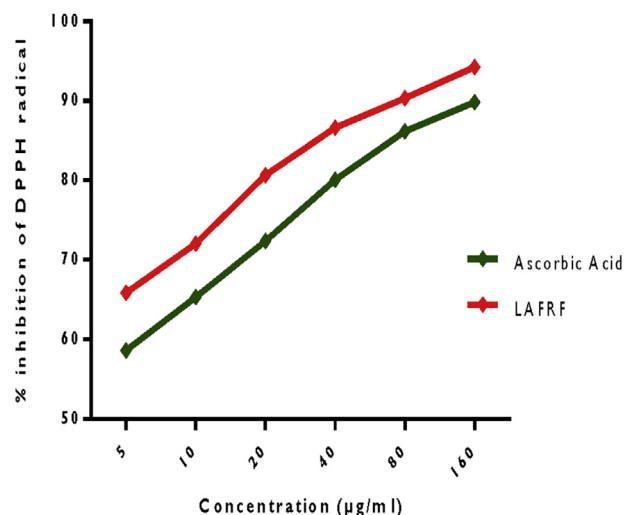


Figure 3. DPPH radical scavenging activity of the LAFRF.

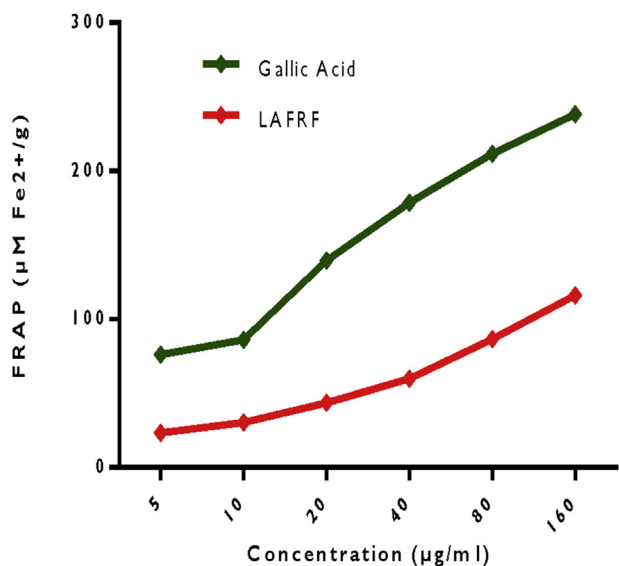


Figure 4. Ferric reducing antioxidant power of the LAFRF.

extraction temperature and the duration of extraction affects the extraction yield of polyphenols (Yi et al., 2012; Li et al., 2014).

### 3.2. Total flavonoid concentration of the LAFRF

The TFC of the LAFRF determined to be  $281.05 \pm 7.44$  mg QE/g of the freeze-dried LAFRF, was remarkably higher when compared to the MELA

( $13.95 \pm 0.65$  mg QE/g). This is consistent with the report of Shodehinde et al. (2017) for the MELA, indicating that solvent partitioning and further purification enhanced the polyphenolic content of the LAFRF.

### 3.3. DPPH radical scavenging activity

The quantitative DPPH radical scavenging activity of the LAFRF shown in Figure 3 indicates a concentration-dependent increase in percentage inhibition of the DPPH radical with an inhibitory concentration at 50% (IC<sub>50</sub>) of  $5.40 \pm 0.00$  μg/ml, when compared to ascorbic acid with an IC<sub>50</sub> of  $7.18 \pm 0.00$  μg/ml. The LAFRF showed significantly ( $p < 0.05$ ) higher scavenging activity for the DPPH radical at all concentrations investigated, when compared to the standard. This indicates a direct radical scavenging relationship between the concentrations and the percentage inhibitions, where the most concentrated sample had the highest percentage inhibition and the least concentrated sample had the least percentage inhibition. The LAFRF displayed rapid discoloration of the purple colored DPPH radical to pale yellow, suggesting a superior electron donating or hydrogen atom-donating ability so as to stabilize the highly reactive DPPH radical. The degree of discoloration is proportional to the concentration and potency of the antioxidants in the LAFRF, particularly the flavonoids which scavenge the DPPH radical. This finding is consistent with the report of Atiko et al. (2016) who suggested that phenolic compounds in *L. africana* may be responsible for the DPPH radical scavenging activity of the plant. Flavonoids like quercetin, isorhamnetin, luteolin and rutin identified in LAFRF has been shown to be potent radical scavengers and reducing agents, due to their ability donate hydrogen atom as well as transfer of electron and protons (Garayev et al., 2018).

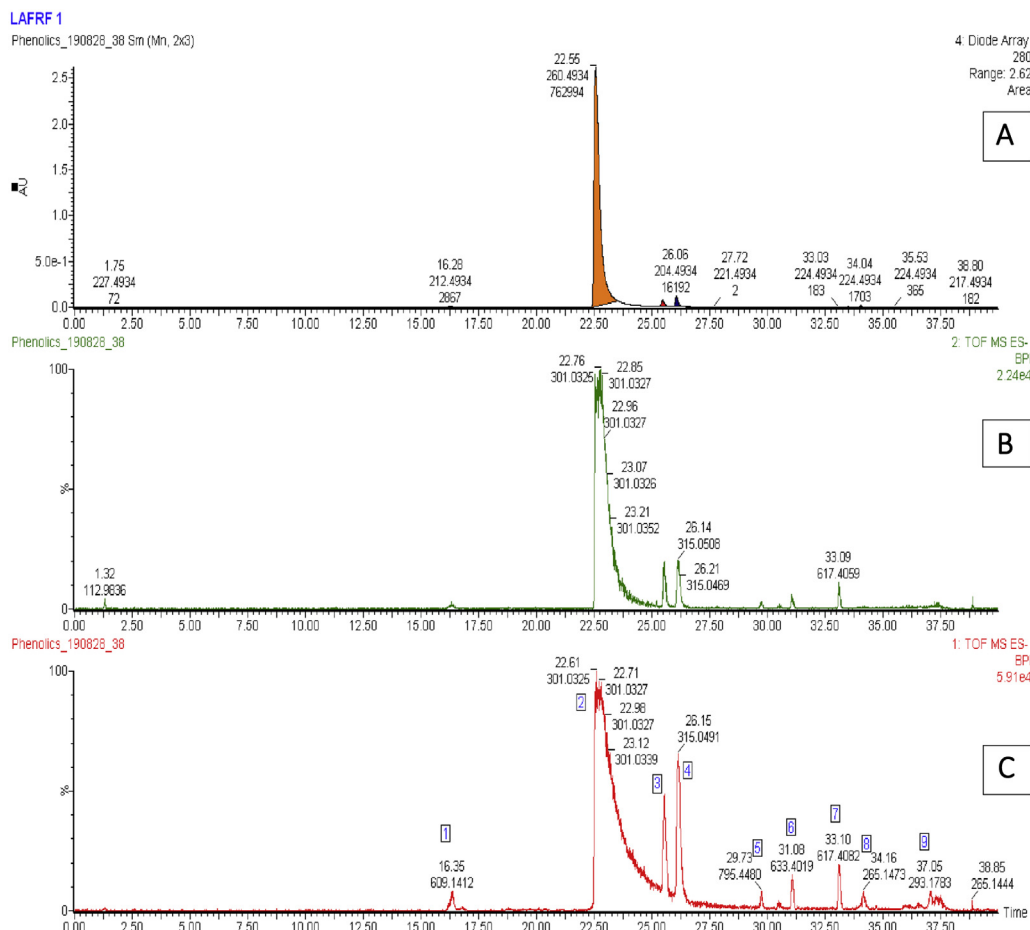
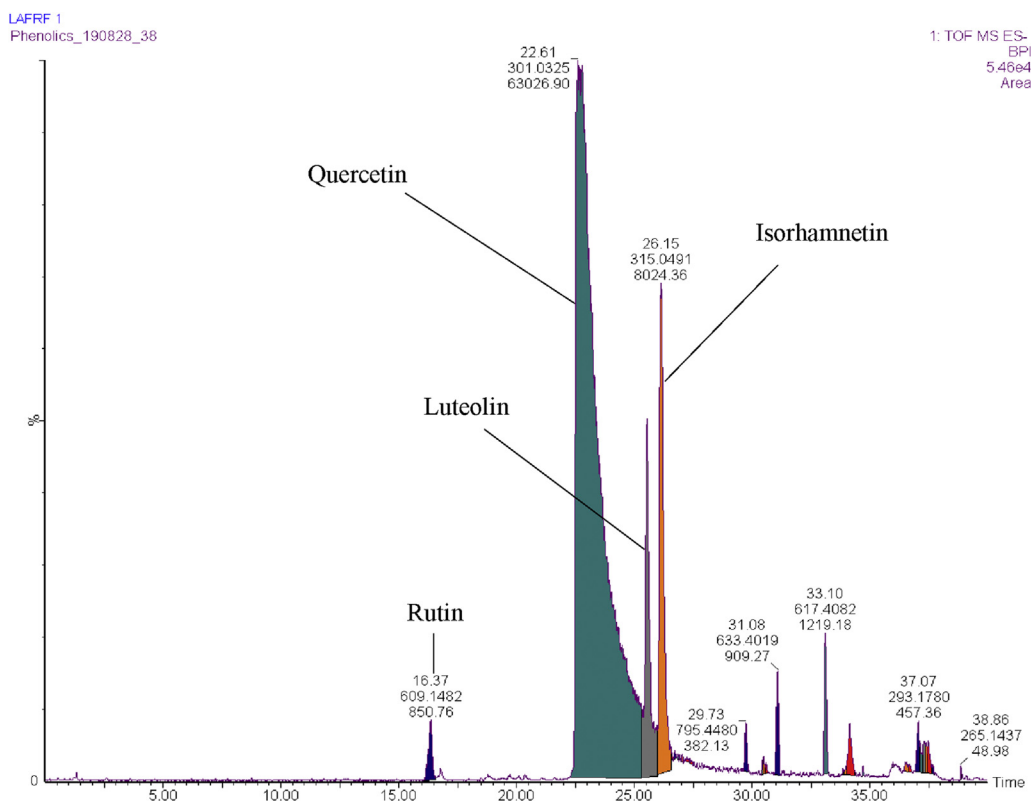


Figure 5. Overlay of UV-PDA 280 nm (A), and base peak intensity (BPI) chromatograms (B and C) of the LAFRF.



**Figure 6.** UPLC-QTOF-ESI-MS/MS fingerprint of LAFRF showing retention time, molecular mass and peak area.

### 3.4. Ferric reducing antioxidant potential

The FRAP of the LAFRF and the standard reported in Figure 4, showed a concentration-dependent increase in the ferric reducing power of the LAFRF and gallic acid standard. From the result obtained, the FRAP of gallic acid was observed to be significantly ( $p < 0.05$ ) higher when compared to that of the LAFRF. The presence of reducing agents such as flavonoids in the LAFRF were able to reduce  $Fe^{3+}$  to  $Fe^{2+}$  which is a more useful form of iron for cellular processes. The mechanism of reduction involves breaking down of free radical chain reaction by donating a hydrogen atom (Anosike et al., 2019). The FRAP displayed by the LAFRF indicates its effectiveness in reducing the transition state of iron, and decrease in the rate of free radical generation through the Fenton reaction. Compounds with reducing power possess good electron donating ability, and can reduce oxidized intermediates of lipid peroxidation by acting as primary and secondary antioxidants (Chanda and Dave, 2009). From our results, the flavonoids in the LAFRF showed potency to donate electrons to the reactive  $Fe^{3+}$  radicals, converting them into stable non-reactive species and terminating the free radical chain reaction.

### 3.5. Fourier transformed infrared spectroscopy

In order to identify the type of chemical bonds and the functional groups present in the LAFRF, FTIR spectroscopy was carried out (Figure B.1). The spectrum indicated presence of very strong (vs), and

strong (s) molecular vibrations at  $3059\text{--}3820\text{ cm}^{-1}$  indicating the presence of multiple broad and free hydroxyl ( $-\text{OH}$ ) stretching,  $1704\text{--}2221\text{ cm}^{-1}$  ( $\text{C}=\text{C}-\text{H}$ ,  $\text{C}=\text{CH}$ ,  $\text{Ar}-\text{H}$ ,  $\text{C}-\text{H}$  stretch),  $1624\text{ cm}^{-1}$  (aromatic  $\text{C}=\text{C}$  bend,  $\text{OH}$  from phenols, flavones, and conjugated benzene ring structures),  $1315\text{ cm}^{-1}$  ( $\text{C}-\text{O}-\text{C}$ ,  $\text{C}=\text{O}$  and  $-\text{OH}$  stretching),  $1474\text{ cm}^{-1}$  ( $\text{OH}$  from phenols,  $\text{CH}_2$  and  $\text{CH}_3$ ,  $\text{C}-\text{H}$ ,  $\text{R}-\text{CH}_2\text{CH}_3$ ).

### 3.6. UV analysis of the LAFRF by UPLC-PDA detection

The UV-visible spectrum (Figure B.2) showed one peak at  $370.5\text{ nm}$ , corresponding to band II absorption, indicative of a flavonol. The qualitative UPLC-PDA spectral analysis of the LAFRF (photodiode array channels) (Figures 7, 8, 9, and 10) showed two peaks at  $240\text{--}285\text{ nm}$  (band II), and  $320\text{--}385\text{ nm}$  (band I) which are characteristic absorption maxima for flavones and flavonol class of flavonoids and their derivatives. The band I is considered to be associated with absorption due to the B-ring cinnamoyl system, while the band II absorption is indicative of the benzoyl system of the A-ring (Gupta et al., 2016). The precise position and relative intensities of these maxima give valuable information on the nature and type of flavonoids present. Thus, the UV spectrum of the LAFRF is indicative of the presence of flavones and flavonols class of flavonoids. Consequently, these subclass cannot be fully characterized by UPLC-PDA spectral analysis only, hence we further characterized the LAFRF by UPLC-PDA-QTOF-ESI-MS/MS.

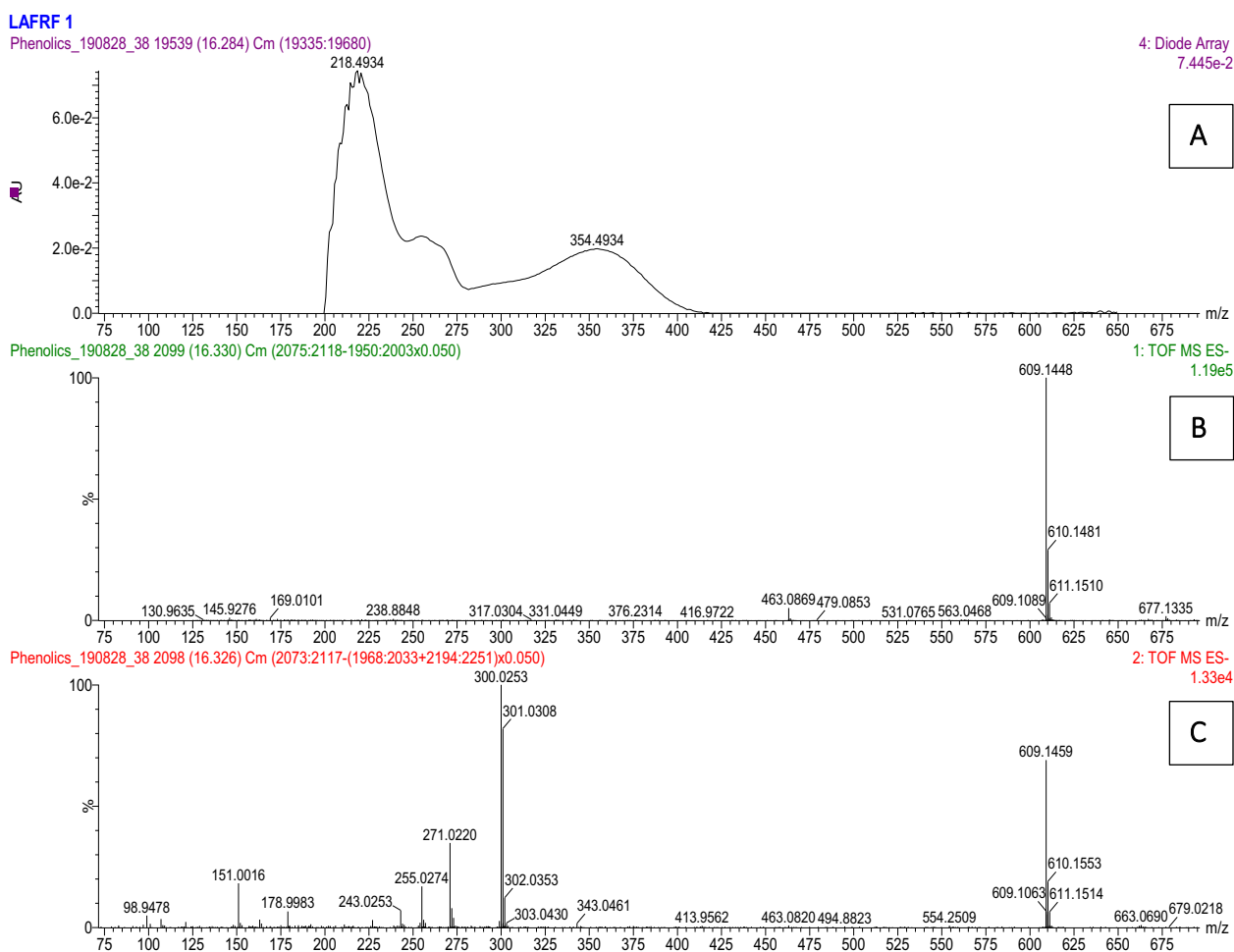
**Table 1.** Structural quantification of the major compounds isolated from the LAFRF.

Major Peaks LAFRF Flavonoids (95.68%)	Rutin (1.02%)	Quercetin (75.6%)	Luteolin (9.43%)	Isorhamnetin (9.63%)	Minor Peaks Non-phenolic (4.32%)
Concentration (mg/kg)	17540.4	758983.6	126524.3	197949.0	ND
Concentration (g/100g)	1.75	75.90	12.65	19.79	ND
Peak Areas	850.76	63026.90	7861.69	8024.36	3016.92

Compounds were quantified semi-quantitatively against a rutin calibration standard. ND (Not determined).

**Table 2.** Characterization of compounds identified from the LAFRF using UPLC-PDA-QTOF-ESI-MS/MS.

Peak	Retention Time	<sup>a</sup> m/z	<sup>b</sup> [M-H] <sup>-</sup>	<sup>c</sup> MS <sup>E</sup> (MS/MS)	UV-Maxima (nm)	Identification	Area (%)
1	16.37	609.145	C <sub>27</sub> H <sub>29</sub> O <sub>16</sub>	301, 271, 255, 243, 178, 151	254 and 354	Quercetin-3-O-rutinoside (Rutin)	1.02
2	22.61	301.033	C <sub>15</sub> H <sub>9</sub> O <sub>7</sub>	299, 273, 229, 180, 178, 152, 121, 107	254 and 370	5,7,3',4'-flavan-3-ol (Quercetin)	75.60
3	25.55	285.038	C <sub>15</sub> H <sub>9</sub> O <sub>6</sub>	259, 229, 187, 178, 151, 121, 107	264 and 366	3',4',5,7-tetrahydroxyflavone (Luteolin)	9.42
4	26.15	315.049	C <sub>16</sub> H <sub>11</sub> O <sub>7</sub>	300, 271, 255, 227, 178, 151, 148, 107	254 and 370	Quercetin 3-methyl ether (Isorhamnetin)	9.63
5	29.73	795.452	C <sub>42</sub> H <sub>67</sub> O <sub>14</sub>	765, 615, 555, 437, 325, 301, 183, 151, 119	Non UV	Soyasaponin III (1-) ion	0.46
6	31.08	633.401	C <sub>36</sub> H <sub>57</sub> O <sub>9</sub>	557, 541, 457, 409, 375, 339, 301, 271, 197, 183, 151, 113	Non UV	Soyasapogenol-B-3-O-β-glucuronate	1.09
7	33.10	617.406	C <sub>36</sub> H <sub>57</sub> O <sub>8</sub>	579, 454, 439, 397, 339, 301, 255, 183, 113	Non UV	Oleanolate-3-O-β-D-glucoside	1.46
8	34.16	265.146	Nil	222, 184, 183, 100, 98, 96	224	Unknown	0.10
9	37.07	293	Nil	265, 248, 221, 183, 150	Non UV	Unknown	0.11
10	38.86	265	Nil	Not detected	Non UV	Unknown	0.06

<sup>a</sup> Accurate mass detection.<sup>b</sup> Negative ions.<sup>c</sup> Mass fragmentation patterns with intensity normalised to 100 for the highest fragment.**Figure 7.** UV (A), unfragmented (B) and fragmented (C) mass spectra for the rutin peak at 16.3 min.

### 3.7. Identification and characterization of the LAFRF

High resolution UPLC-PDA-QTOF-ESI-MS/MS was used for identification, characterization and structure elucidation of compounds isolated from the LAFRF. The UPLC-PDA (280 nm), and QTOF-ESI-MS/MS fingerprints were generated (Figures 5 and 6). The constituent flavonoids were subsequently analyzed by ESI-MS<sup>1</sup> and MS<sup>2</sup> with characteristics shown in Tables 1 and 2. Electrospray ionization (ESI) was used in the negative mode ( $m/z$  values  $[M - H]^-$ ) to provide accurate mass detection

and fragmented data (MS<sup>2</sup>) of the identified compounds in the LAFRF listed in Table 2. Relative identifications were made from the respective UV maxima spectra obtained from the photodiode array channel (280 nm), retention times, accurate mass detection, fragmentation patterns, and MS library information with further confirmations from literature.

The UPLC-PDA-QTOF-ESI-MS/MS fingerprint of the LAFRF (Figures 5 and 6) detected the presence of 7 compounds based on their various ultraviolet absorption band (UV maxima), retention times, peak areas,  $m/z$ ,  $[M - H]^-$  and library identifications, of which 4 compounds formed the

major peaks. They were identified, quantified semi-quantitatively against a Rutin calibration standard, and structurally characterized. These are: Quercetin, 758983.6 mg/kg (75.6%) >> Quercetin 3-methyl ether, 197949.0 mg/kg (9.63%) > Luteolin, 126524.3 mg/kg (9.42%) > Rutin, 17540.4 mg/kg (1.02%), making up 95.68% of polyphenolic bioactive compounds in the LAFRF. The other 6 compounds which constitutes the minor peaks made up a total of 4.32%. Compound 1 was eluted at retention time (Rt) 16.33 min and exhibited UV maxima from the photodiode array channel at 254 nm and 354 nm (Figure 7). The mass ionization signal  $[M-H]^-$  ion ( $m/z$  609.145), and molecular formula ( $C_{27}H_{29}O_{16}$ ) was generated. The mass fragmentation patterns with intensity normalized to 100 for the highest fragment resulted in a quercetin fragment at 301 (100), and fragment ion masses  $m/z$  of 271, 255, 243, 178, 151. The compound was identified as quercetin-3-O-rutinoside (Rutin), a flavonoid glycoside which combines the flavonol, quercetin; and a disaccharide, rutinose ( $\alpha$ -L-rhamnopyranosyl-(1-6)- $\beta$ -D-glucopyranose). The compound has been previously identified from the plant by (Shodehinde et al., 2017), and is in agreement with the identification by Zhou et al. (2018). Quantification of compound 1 (Rutin) using the standard calibration curve of Rutin showed its concentration in the LAFRF to be 17540.4 mg/kg, with total peak area of 1.02%.

Compound 2, eluted at 22.61 min and indicated UV maxima at 254 nm and 370 nm (Figure 8). The  $[M-H]^-$  ion was  $m/z$  301.033, with molecular formula of  $C_{15}H_9O_7$ . The mass fragmentation patterns generated were  $m/z$  299, 273, 229, 180, 178, 152, 121, 107, for different compounds fragmented from the parent flavonoid identified. The compound was identified as 5, 7, 3', 4'-flavan-3-ol (Quercetin) which is consistent with the identifications of Oufir et al. (2015), Li et al. (2016a), and Garayev et al. (2018). Quantification of compound 2 using a standard Rutin calibration plot showed compound 2 to be present in the highest concentration (758983.6 mg/kg), with a total peak area of

75.6%. Compound 3, eluted at 25.44 min showed UV maxima at 264 nm and 366 nm (Figure 9), which is characteristic of flavones showing parent ions of  $m/z$  285.038  $[M-H]^-$  with molecular formula of  $C_{15}H_9O_6$ , and fragment ions of  $m/z$  259, 229, 187, 178, 151, 121, indicating an aglycone flavone identified as 3',4',5,7-tetrahydroxyflavone (Luteolin). The structure of compound 3 showed similar fragmentation patterns from the parent compound with those reported by Stander et al. (2017), and Garayev et al. (2018). The concentration of compound 3 (Luteolin) in the LAFRF was 126524.3 mg/kg, with peak area of 9.42%.

Compound 4 was eluted at 26.12 min with UV maxima of 254 nm and 370 nm (Figure 10), which is characteristic of a flavonol showing parent ions of  $m/z$  315.049  $[M-H]^-$ , with molecular formula of  $C_{16}H_{11}O_7$ . The mass fragmentation patterns with intensity normalized to 100 for the highest fragment resulted in a quercetin fragment at 300 (100), and fragment ions of  $m/z$  271, 255, 227, 178, 151, 148, 107, indicating an aglycone flavonol identified as quercetin 3-methyl ether (Isorhamnetin), seeing that it fragments to give a quercetin fragment. The concentration of Isorhamnetin in the LAFRF was 197949.0 mg/kg (9.63%), with total peak area of 9.63%.

Compounds 5, 6 and 7 identified in the LAFRF are non-phenolic compounds, and they make up the minor peaks. They exhibited no characteristic absorption for phenolic compounds at ultraviolet region (PDA\_280 nm). Compound 5, identified as soyasaponin III (1-) ion, is a triterpenoid which retained in the LC column at 29.3 min, and displayed mass fragmentation patterns of 765, 615, 555, 437, 325, 301, 183, 151 and 119. The compound indicated  $m/z$  795.452  $[M-H]^-$ , with molecular formula of  $C_{16}H_{11}O_7$  (Table 2, Figure C.1). Compound 6, identified as Soyasapogenol-B-3-O- $\beta$ -glucuronate, is a monocarboxylic acid anion which retained at 31.08 min, showing fragment ions of 557, 541, 457, 409, 375, 339, 301, 271, 197, 183, 151 and 113, with  $m/z$  633.401  $[M-H]^-$  and a molecular formula of  $C_{35}H_{57}O_9$  (Table 2, Figure C.2).

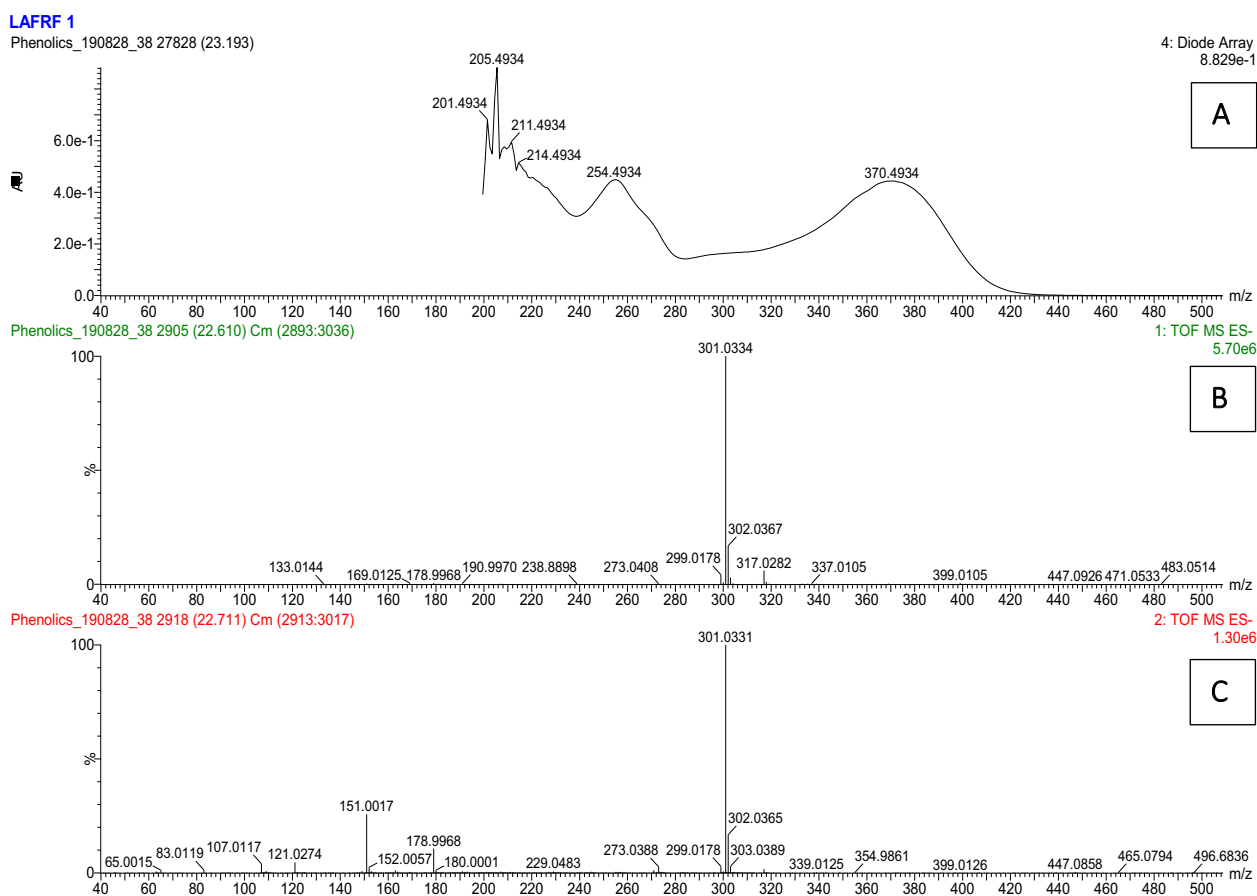


Figure 8. UV (A), unfragmented (B) and fragmented (C) mass spectra for quercetin peak at 22.6 min.



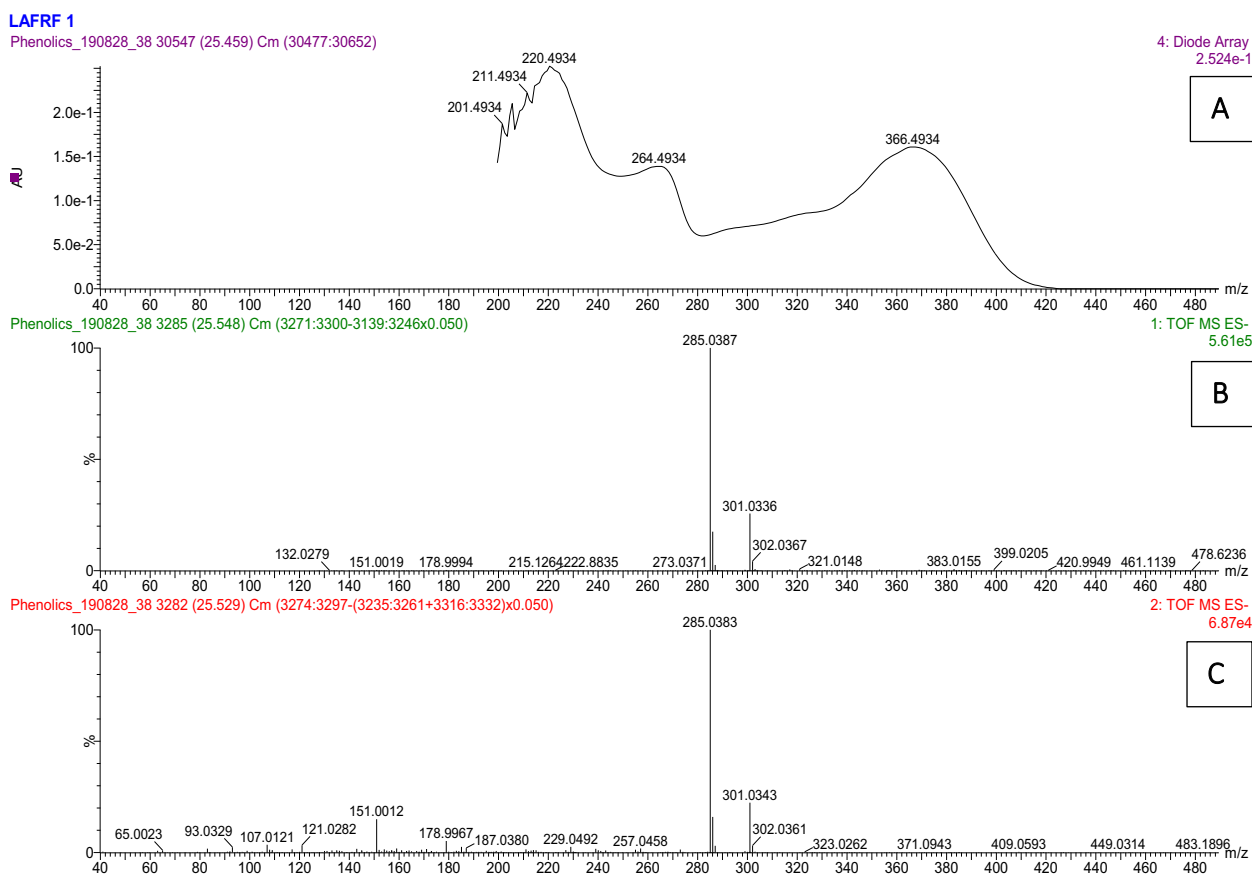


Figure 9. UV (A) unfragmented (B) and fragmented (C) mass spectra for luteolin peak at 25.5 min.

Compound 7, identified as Oleanolate-3-O- $\beta$ -D-glucoside is also a monocarboxylic acid anion which indicated a retention time of 33.10 min. The mass spectral data of compound 7 generated fragment ions of 579, 454, 439, 397, 339, 301, 255, 183, 113, with  $m/z$  617.406  $[M-H]^-$ , and a molecular formula of  $C_{36}H_{57}O_9$  (Table 2, Figure C.3). The UPLC-PDA-QTOF-ESI-MS/MS analysis of the LAFRF also indicated the presence of unknown compounds in peaks 8 (Figure C.4), and 9 (Figure C.5). The UPLC-PDA-QTOF-ESI-MS/MS method used in this study has been demonstrated to be an accurate and effective tool for analysis of polyphenolic components in a complex plant extract.

### 3.8. Effect of the LAFRF on renal function indices of $CCl_4$ -intoxicated rats

Urea, a nitrogenous end product of protein catabolism, is one of the waste product of the body which is passed into the blood stream to be removed by the kidneys through urine. Creatinine on the other hand is a waste product formed by spontaneous dehydration of the kidneys and usually produced in the body in proportion to body mass. Measurement of serum urea and creatinine concentrations serve as useful biomarkers for assessing the functionality of the kidneys in a diseased state. In the present study,  $CCl_4$  intoxication led to a significant ( $p < 0.05$ ) increase in serum urea and creatinine concentrations as observed in the  $CCl_4$  control group when compared to the normal control (Table 3). This effect could be as a result of oxidative damage to the kidneys caused by  $CCl_4$  bio-activation, lipid peroxidation, or increase in breakdown of intracellular membrane proteins, muscle mass or creatinine phosphate of the  $CCl_4$  control rats, thus signifying a possible impairment in kidney function, and a resultant increase in the levels of urea and creatinine, as the kidneys are not able to remove them from the blood. This finding agrees with El-haskoury et al. (2018), who also reported significant ( $p < 0.05$ )

elevation in urea and creatinine concentrations following  $CCl_4$  administration to rats.

Carbon tetrachloride is highly toxic to the kidneys just as it is to the liver, with a similar mechanism of toxicity. However,  $CCl_4$  shows a high affinity to the kidney cortex which is predominant in cytochrome P-450 (Jaramillo-juarez et al., 2008). Due to the renal injury caused by  $CCl_4$  bio-activation, the transport function of the nephrotic cells becomes altered, leading to impaired kidney functions. Treatment with the LAFRF at doses of 3, 10 and 30 mg/kg b.w., in the preventive and curative studies resulted in a significantly ( $p < 0.05$ ) lower urea and creatinine concentrations, indicating a return to normal kidney function. This is in line with the study of Dahal and Mulukuri (2015), who stated that flavonoids like silymarin, hesperedin, morin hydrates, propinol, naringenin, quercetin, and rutin have protective effect on the kidneys following chemically-induced kidney failure. The ability of the total flavonoids in the LAFRF to alleviate renal toxicity could be attributed to the presence of polyphenols such as quercetin, isorhamnetin, rutin, and luteolin identified in the LAFRF. These antioxidant polyphenols are able to directly scavenge radical species generated by  $CCl_4$ , and prevent lipid peroxidation, thus protecting the kidney tissues against oxidative damage and loss of kidney function (Lien et al., 2012). The administration of various natural or synthetic antioxidants has been shown to be beneficial in the prevention and attenuation of renal injuries in numerous animal models of kidney diseases. Tunçdemir et al. (2018), reported the renoprotective effect of quercetin on diabetic nephropathy in rats. Luteolin and other natural flavonoids have been reported to have antioxidative and renoprotective effects (Arslan et al., 2016; Kalbolandi et al., 2019).

The effect of the LAFRF on serum electrolyte concentrations of  $CCl_4$ -intoxicated rats (Table 3), also indicated a significant ( $p < 0.05$ ) increase in the concentrations of serum  $Na^+$ ,  $K^+$ , and  $Cl^-$  of the  $CCl_4$  control, relative to the normal control rats. This further indicated altered

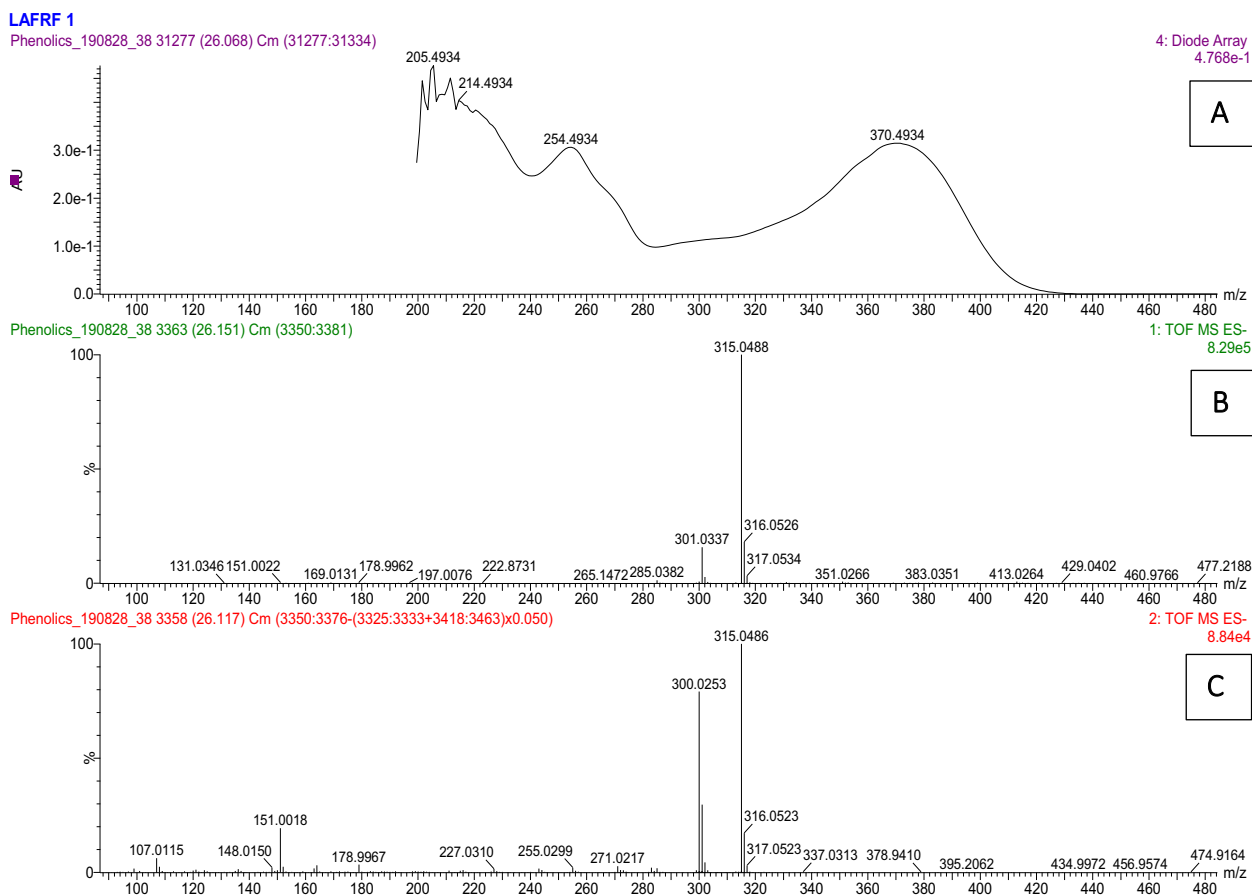


Figure 10. UV (A), unfragmented (B) and fragmented (C) mass spectra for isorhamnetin peak at 26.12 min.

Table 3. Effect of LAFRF on serum urea, creatinine and electrolyte concentrations of CCl<sub>4</sub>-intoxicated rats.

Groups	Treatments	Urea (mg/dl)	Creatinine (mg/dl)	Na <sup>+</sup> (mmol/l)	K <sup>+</sup> (mmol/l)	Cl <sup>-</sup> (mmol/l)
1	Normal control	66.40 ± 1.95 <sup>a</sup>	2.44 ± 0.23 <sup>a, b</sup>	213.00 ± 16.51 <sup>d</sup>	4.24 ± 0.15 <sup>a, b</sup>	96.00 ± 0.71 <sup>a</sup>
2	CCl <sub>4</sub> control	83.20 ± 2.17 <sup>b</sup>	3.06 ± 0.09 <sup>c</sup>	233.80 ± 13.37 <sup>e</sup>	5.20 ± 0.10 <sup>d</sup>	107.60 ± 3.29 <sup>b</sup>
4A	10 mg/kg b.w. LAFRF + CCl <sub>4</sub>	73.20 ± 2.28 <sup>d, e</sup>	2.32 ± 0.16 <sup>a, e</sup>	179.80 ± 7.01 <sup>a, b</sup>	4.30 ± 0.43 <sup>b</sup>	96.60 ± 0.89 <sup>a</sup>
5A	30 mg/kg b.w. LAFRF + CCl <sub>4</sub>	76.80 ± 2.39 <sup>e</sup>	2.27 ± 0.10 <sup>a, e</sup>	183.00 ± 6.96 <sup>b</sup>	4.04 ± 0.42 <sup>a, b</sup>	97.00 ± 1.00 <sup>a</sup>
6A	100 mg/kg b.w. AA + CCl <sub>4</sub>	68.80 ± 4.60 <sup>a, d</sup>	1.53 ± 0.20 <sup>f</sup>	181.00 ± 10.68 <sup>a, b</sup>	4.44 ± 0.32 <sup>b, c</sup>	95.80 ± 0.84 <sup>a</sup>
3B	CCl <sub>4</sub> + 3 mg/kg b.w. LAFRF	67.80 ± 4.87 <sup>a</sup>	2.58 ± 0.41 <sup>a, b</sup>	209.20 ± 2.17 <sup>d</sup>	4.16 ± 0.54 <sup>a, b</sup>	97.00 ± 0.71 <sup>a</sup>
4B	CCl <sub>4</sub> + 10 mg/kg b.w. LAFRF	57.60 ± 6.02 <sup>f</sup>	2.10 ± 0.22 <sup>d, e</sup>	201.80 ± 8.64 <sup>c, d</sup>	5.06 ± 0.17 <sup>d</sup>	96.20 ± 1.30 <sup>a</sup>
5B	CCl <sub>4</sub> + 30 mg/kg b.w. LAFRF	64.80 ± 4.32 <sup>a</sup>	2.32 ± 0.26 <sup>a, e</sup>	167.80 ± 6.22 <sup>a</sup>	4.32 ± 0.66 <sup>b</sup>	97.40 ± 1.14 <sup>a</sup>
6B	CCl <sub>4</sub> + 100 mg/kg b.w. AA	76.60 ± 2.19 <sup>c</sup>	2.68 ± 0.11 <sup>b</sup>	192.40 ± 11.93 <sup>b, c</sup>	4.88 ± 0.08 <sup>c, d</sup>	97.20 ± 0.45 <sup>a</sup>

Results are expressed as mean ± standard deviation; n = 5. Mean values with different alphabets as superscripts when compared with groups down the columns are considered significant at  $p < 0.05$ . AA (L-ascorbic acid standard).

kidney functions arising from CCl<sub>4</sub> toxicity on the renal-tubular system, and corroborates well with previous studies by Awodele et al. (2015), and Ayanniyi et al. (2017), on renal damage following CCl<sub>4</sub> induction. This effect could be accrued to the ability of the toxic and reactive metabolites of CCl<sub>4</sub> to cause oxidative damage to the renal system, leading to increased concentration of the electrolytes in the blood as noticed in the CCl<sub>4</sub> control group. Treatment with the LAFRF in the preventive and curative studies attenuated the cytotoxic effects of CCl<sub>4</sub>, and caused a significant ( $p < 0.05$ ) decrease in glomerular filtration by restoring the concentration of electrolytes to normal levels similar to those seen in the normal control group. The decline in Na<sup>+</sup>, K<sup>+</sup> and Cl<sup>-</sup> concentrations which is reported to be treatment related, and noticed in the LAFRF treated groups, is in line with the studies of Okokon et al. (2011), Awodele et al. (2015), and Ayanniyi et al. (2017). From the data

obtained, it is possible to speculate that the antioxidant property of the LAFRF is responsible for its reno-modulatory effects. The constituent total flavonoids isolated from the LAFRF have shown remarkable antioxidant activities *in vitro*, and could be responsible for the observed renoprotective effects recorded in this study, either by the inhibition of the production of ROS and/or the sequestration of the ROS produced by CCl<sub>4</sub>, thus protecting against its damaging effects (Konda et al., 2016).

### 3.9. Effect of the LAFRF on biomarkers of cardiac function of CCl<sub>4</sub>-intoxicated rats

The heart is one of the key organs in the body which is also subject to oxidative damage following exposure to chemical and environmental toxicants such as CCl<sub>4</sub>. This is because the cardiac tissue has affinity for

**Table 4.** Effect of LAFRF on serum and heart tissue LDH and CK activities of CCl<sub>4</sub>-intoxicated rats.

Groups	Treatments	Tissue LDH (IU/L)	Serum LDH (IU/L)	Tissue CK (IU/L)	Serum CK (IU/L)
1	Normal Control	10.25 ± 0.00 <sup>a</sup>	21.34 ± 2.31 <sup>a</sup>	11.44 ± 1.60 <sup>a</sup>	8.37 ± 0.93 <sup>a</sup>
2	CCl <sub>4</sub> Control	65.23 ± 1.12 <sup>b</sup>	52.35 ± 2.44 <sup>b</sup>	28.88 ± 0.00 <sup>b</sup>	23.53 ± 1.82 <sup>b</sup>
3A	3 mg/kg b.w. LAFRF + CCl <sub>4</sub>	16.74 ± 0.77 <sup>c</sup>	37.23 ± 1.03 <sup>c</sup>	24.21 ± 3.03 <sup>c</sup>	20.96 ± 0.60 <sup>c</sup>
4A	10 mg/kg b.w. LAFRF + CCl <sub>4</sub>	16.19 ± 0.00 <sup>c</sup>	29.44 ± 1.16 <sup>d</sup>	20.39 ± 1.68 <sup>d</sup>	16.93 ± 0.71 <sup>d</sup>
5A	30 mg/kg b.w. LAFRF + CCl <sub>4</sub>	19.38 ± 1.51 <sup>d</sup>	25.42 ± 5.77 <sup>e</sup>	19.42 ± 1.20 <sup>d</sup>	11.37 ± 1.21 <sup>e</sup>
6A	100 mg/kg b.w. AA + CCl <sub>4</sub>	29.40 ± 1.51 <sup>e</sup>	23.90 ± 1.37 <sup>a, e</sup>	11.35 ± 1.46 <sup>a</sup>	9.43 ± 0.74 <sup>a</sup>
3B	CCl <sub>4</sub> + 3 mg/kg b.w. LAFRF	24.60 ± 3.14 <sup>d</sup>	46.82 ± 1.74 <sup>f</sup>	21.42 ± 1.56 <sup>c, d</sup>	17.63 ± 1.18 <sup>d, f</sup>
4B	CCl <sub>4</sub> + 10 mg/kg b.w. LAFRF	17.38 ± 1.68 <sup>f</sup>	40.21 ± 3.04 <sup>e</sup>	22.69 ± 0.00 <sup>e</sup>	17.27 ± 1.14 <sup>d</sup>
5B	CCl <sub>4</sub> + 30 mg/kg b.w. LAFRF	18.41 ± 0.22 <sup>f</sup>	39.07 ± 3.63 <sup>e</sup>	18.26 ± 2.93 <sup>d</sup>	16.86 ± 1.15 <sup>d</sup>
6B	CCl <sub>4</sub> + 100 mg/kg b.w. AA	22.62 ± 3.03 <sup>d</sup>	38.39 ± 2.93 <sup>c</sup>	17.50 ± 1.95 <sup>d</sup>	18.97 ± 1.70 <sup>f</sup>

Results are expressed as mean ± standard deviation; n = 5. Mean values with different alphabets as superscripts when compared with groups down the columns are considered significant at  $p < 0.05$ . AA (L-ascorbic acid standard).

CCl<sub>4</sub> due to the activities of the cytochrome P-450 oxygenase system which triggers the bio-activation of CCl<sub>4</sub> leading to oxidative degradation of membrane phospholipids and proteins of the heart tissues, as well as disruption and loss of the cardiac cell membrane integrity (Khan and Ahmed, 2009). In this study, CCl<sub>4</sub> intoxication caused a marked increase in the activities of serum and heart tissue CK and LDH as observed in the CCl<sub>4</sub> control group, relative to the normal control (Table 4). This sharp elevation in the activities of CK and LDH agrees with the report of Njoku et al. (2017), and is indicative of damage to the myocardial cell membrane, and a consequent leakage of cytosolic contents of the cell into the circulation. Daily oral administration of graded doses of the LAFRF and the standard, led to significant ( $p < 0.05$ ) declines in the activities of these cardioprotective enzymes near normal, in a dose dependent manner both in the preventive and curative studies, hence, ameliorating the cytotoxic effect of CCl<sub>4</sub> on the heart tissue.

The ability of the LAFRF to ameliorate the toxic effects of CCl<sub>4</sub> suggests its protective effect on the myocardium. This cardioprotective effect could be attributed to the ability of the total flavonoids in the LAFRF, to chelate the by-products of CCl<sub>4</sub> metabolism, hence, scavenging the ROS generated. Moreover, the total flavonoids in the LAFRF have been reported to possess cardioprotective effect. Quercetin, identified in highest quantity in the LAFRF has been reported to have therapeutic effect on cardiovascular diseases due to its antioxidant activity. A recent study showed that oxidative stress is an important factor involved in the development of acute myocardial infarction (Xu et al., 2019). Li et al. (2016b) reported that quercetin effectively protected against myocardium injury. In addition, quercetin protects the heart from secondary cardiac dysfunction due to oxidative stress and inflammation by significantly attenuating overproduction of ROS, decreased trauma-induced damage, increased TNF- $\alpha$ , and prevents Ca<sup>2+</sup> overload-induced myocardial cell injury, indicating its efficiency in preventing cardiac injury induced by oxidative stress (Jing et al., 2016). A recent study by Lin et al. (2018) reported the cardioprotective effects of rutin via the upregulation of the selective SIRT1/Nrf2 signaling. Wang et al. (2017), also reported the cardioprotective effects of rutin by significantly reducing CK, LDH, troponin T levels in rats following exposure to pirarubicin. Luteolin, a flavonoid also isolated from the LAFRF in this study, has been previously reported to exert cardioprotective effects *in vivo*, by improving the sarcoplasmic reticulum Ca<sup>2+</sup>-ATPase activity during ischemic reperfusion in rats as well as through multiple molecular mechanisms (Luo et al., 2017). Cumulatively, we can speculate that the total flavonoids in the LAFRF functioned in synergism and/or potentiation towards improving the cardiac function of the treated rats.

#### 4. Conclusion

In this study, we showed that the leaves of *L. africana*, is a good source of polyphenolic phytochemicals. The bioactive compounds isolated from

the plant leaves, identified and characterized by UPLC-PDA-QTOF-ESI-MS/MS method exhibited remarkably high antioxidant activities due to their synergistic and/or additive effects in sequestering free radicals *in vitro*. The LAFRF also displayed remarkable improvements in renal and cardiac functions of CCl<sub>4</sub>-intoxicated rats *in vivo*, suggesting its potential as an alternative source for the development of biopharmaceutical agent(s) useful in the treatment and management of oxidative stress-related diseases and complications, particularly those with the etiology of lipid peroxidation.

#### Declarations

##### Author contribution statement

D.E. Ekpo: Conceived and designed the experiments; Performed the experiments; Analyzed and interpreted the data; Contributed reagents, materials, analysis tools or data; Wrote the paper.

P.E. Joshua: Conceived and designed the experiments; Analyzed and interpreted the data; Contributed reagents, materials, analysis tools or data.

J.O. Ogidigo: Performed the experiments; Analyzed and interpreted the data; Contributed reagents, materials, analysis tools or data.

O.F.C. Nwodo: Conceived and designed the experiments; Analyzed and interpreted the data.

##### Funding statement

This research did not receive any specific grant from funding agencies in the public, commercial, or not-for-profit sectors.

##### Competing interest statement

The authors declare no conflict of interest.

##### Additional information

Supplementary content related to this article has been published online at <https://doi.org/10.1016/j.heliyon.2020.e04154>.

##### Acknowledgements

The authors are thankful to Dr. Udofia A. Obot (PhD), of the Century Recovery Services Ltd., Abuja, Nigeria, for providing preliminary resources for the conduct of this research. We are also very grateful to Dr. Malcolm J. C. Taylor (PhD), of the Mass Spectrometry Unit, Central Analytical Facility (CAF), Stellenbosch University, South Africa, for conducting the UPLC-PDA-QTOF-ESI-MS/MS analysis, and Dr. Olaposi I. Omotuyi (PhD), of the Centre for Bio-computing and Drug Design

(CBDD), Adekunle Ajasin University, Akungba, Nigeria, for providing a suitable laboratory bench work space for the isolation and purification of the LAFRF. The laboratory assistance of Mr. Prince O. James & Mr. Alpha C. Chukwunelo is well appreciated.

## References

- Andy, I.E., Eja, M.E., Mboro, C.I., 2008. An evaluation of the antimicrobial potency of *Lasianthera africana* (Beauv) and *Heinsia crinata* (G. Taylor) on *Escherichia coli*, *Salmonella typhi* *Staphylococcus aureus* and *Candida albicans*. *Malay. J. Microbiol.* 4 (1), 25–29.
- Anosike, C.A., Igboegwu, O.N., Nwodo, O.F.C., 2019. Antioxidant properties and membrane stabilization effects of methanol extract of *Mucuna pruriens* leaves on normal and sickle erythrocytes. *J. Tradit. Complement. Med.* 9, 278–284.
- Arslan, B.Y., Arslan, F., Erkalp, A.A., Sevdı, M.S., Yıldız, G., Küçük, S.H., Altınay, S., 2016. Luteolin ameliorates colistin-induced nephrotoxicity in the rat models. *Renal Fail* 38 (10), 1735–1740.
- Atiko, R., Onocha, P.A., Oyedemi, S.O., 2016. Phytochemical analysis and antioxidant properties of *Lasianthera* leaves, stems and roots extracts. *Res. J. Chem. Sci.* 6 (9), 19–26.
- Awodele, O., Adeneye, A.A., Aiyeola, S.A., Benebo, A.S., 2015. Modulatory effect of *Mangifera indica* against carbon tetrachloride induced kidney damage in rats. *Interdiscipl. Toxicol.* 8 (4), 175–183.
- Ayanniji, R.O., Olumoh-Abdul, H.A., Ojuade, F.I., Abdullahi, R., Anafi, S.B., 2017. The protective effect of *Croton zambesicus* against carbon tetrachloride-induced renal toxicity in rats. *Iranian J. Toxicol.* 13 (1), 5–8.
- Bartels, H., Bohmer, M., 1972. *In vitro* determination of creatinine and urea. *Clin. Chem.* 2, 37–193.
- Benzie, I.F.F., Strain, J.J., 1996. The ferric reducing ability of plasma as a measure of antioxidant power: the FRAP assay. *Anal. Biochem.* 239 (1), 70–76.
- Chanda, S., Dave, R., 2009. *In vitro* models for antioxidant activity evaluation and some medicinal plants possessing antioxidant properties: an overview. *Eur. J. Microbiol. Res.* 3, 981–996.
- Chua, L.S., Latiff, N.A., Lee, S.Y., Lee, C.T., Sar-midi, M.R., Aziz, R.A., 2011. Flavonoids and phenolic acids from *Labisia pumila* (Kacip Fatimah). *Food Chem.* 127 (3), 1186–1192.
- Dahal, A., Mulukuri, S., 2015. Flavonoids in kidney protection. *World J. Pharm. Pharmaceut. Sci.* 4 (3), 362–382.
- Ekanem, N.G., Mbagwu, H.O.C., Harry, G.I., 2016. Phytochemical screening and hypoglycaemic activity of *Lasianthera africana* Beauv. (Aquifoliales: Stemonuraceae) leaf extract on diabetic rats. *Braz. J. Biol. Sci.* 3 (6), 293–298.
- El-haskoury, R., Al-Waili, N., Kamoun, Z., Makni, M., Al-Waili, H., Lyoussi, B., 2018. Antioxidant activity and protective effect of carob honey in ccl4-induced kidney and liver injury. *Arch. Med. Res.* 157, 1–8.
- Essien, G.E., Effiong, G.S., 2017. Evaluation of antioxidant potentials in methanol extract of *Gongronema latifolium* and *Lasianthera africana* leaf. *Eur. J. Pharm. Med. Res.* 9 (4), 841–846.
- Garayev, E., Di Giorgio, C., Herbert, G., Mabrouki, F., Chiffolleau, P., Roux, D., Sallan, H., Ollivier, E., Elias, R., Baghdikian, B., 2018. Bioassay-guided isolation and UHPLC-DAD-ESI-MS/MS quantification of potential anti-inflammatory phenolic compounds from flowers of *Inula montana* L. *J. Ethnopharmacol.* 226, 176–184.
- Glantzounis, G.K., Salacinski, H.J., Yang, W., Davidson, B.R., Seifalian, A.M., 2005. The contemporary role of antioxidant therapy in attenuating liver ischemia-reperfusion injury: a review. *Liver Transplant.* 11 (9), 1031–1047.
- Gupta, J., Gupta, A., Gupta, A.K., 2016. Flavonoids: its working mechanism and various protective roles. *Int. J. Chem. Stud.* 4, 190–198.
- Gyamfi, M.A., Yonamine, M., Aniya, Y., 1999. Free scavenging action of medicinal herbs from Ghana: Thonningia sanguine on experimentally-induced liver injuries. *Gen. Pharmacol.* 32 (6), 661–667.
- Jaramillo-Juárez, F., Rodríguez-Vázquez, M.L., Rincón-Sánchez, A.R., Consolación Martínez, M., Ortiz, G.G., Llamas, J., 2008. Acute renal failure induced by carbon tetrachloride in rats with hepatic cirrhosis. *Ann. Hepatol.* 7 (4), 331–338.
- Jing, Z.H., Wang, Z.R., Li, X.J., Li, X.T., Cao, T.T., Bi, Y., Zhou, J.C., Chen, X., Yu, D.Q., Zhu, L., 2016. Protective effect of quercetin on posttraumatic cardiac injury. *Sci. Rep.* 6, 3081235.
- Kalbolandi, S., Gorji, V.A., Babaahmadi-Rezaei, H., Mansouri, E., 2019. Luteolin confers renoprotection against ischemia-reperfusion injury via involving Nrf2 pathway and regulating mir320. *Mol. Biol. Rep.* 46 (4), 4039–4047.
- Khan, M.R., Ahmed, D., 2009. Protective effect of *Digera muricata* (L.) mart on testis against oxidative stress of CCl<sub>4</sub> in rats. *Food Chem. Toxicol.* 47 (6), 1393–1399.
- Konda, V.R., Arunachalam, R., Eerike, M., Rao, K.R., Radhakrishnan, A.K., Raghuraman, L.P., Vinayak, M., Sotiba, D., 2016. Nephroprotective effect of ethanolic extract of *Asima tetraacantha* root in glycerol induced acute renal failure in Wistar albino rats. *J. Tradit. Complement. Med.* 6 (4), 347–354.
- Kumar, P., Mir, S., Semalty, A., 2014. Isolation and characterization of novel flavonoid from methanolic extract of *Pongamia pinnata* Pods. *Res. J. Phytochem.* 8 (1), 21–24.
- Li, P., Yin, Q., Li, S., Huang, X.J., Ye, W.C., Zhang, Q.W., 2014. Simultaneous determination of eight flavonoids and pogostone in *Pogostemon cablin* by high performance liquid chromatography. *J. Liq. Chromatogr. Relat. Technol.* 37 (12), 1771–1784. In this issue.
- Li, Z.H., Guo, H., Xu, W.B., Ge, J., Li, X., Alimu, M., He, D.J., 2016a. Rapid identification of flavonoid constituents directly from PTP1B inhibitory extract of raspberry (*Rubus idaeus* L.) leaves by HPLC-ESI-QTOF-MS-MS. *J. Chromatogr. Sci.* 54 (4), 805–810.
- Li, B., Yang, M., Liu, J.W., Yin, G.T., 2016b. Protective mechanism of quercetin on acute myocardial infarction in rats. *Genet. Mol. Res.* 15, 15017117.
- Lien, E.J., Lien, L.L., Wang, R., Wang, J., 2012. Phytochemical analysis of medicinal plants with kidney protective activities. *Chin. J. Integr. Med.* 18 (10), 790–800.
- Lin, Q., Chen, X.Y., Zhang, J., Yuan, Y.L., Zhao, W., Wei, B., 2018. Upregulation of SIRT1 contributes to the cardioprotective effect of rutin against myocardial ischaemia-reperfusion injury in rats. *J. Funct. Foods.* 46, 227–237.
- Luo, Y., Shang, P., Li, D., 2017. Luteolin: a flavonoid that has multiple cardio-protective effects and its molecular mechanisms. *Front. Pharmacol.* 8, 692–702.
- Manach, C., Morand, C., Crespy, V., Demigne, C., Texier, O., Regerat, F., Remesy, C., 1998. Quercetin is recovered in human plasma as conjugated derivatives which retain antioxidant properties. *FEBS Lett.* 426 (3), 331–336.
- National Academy of Sciences [NAS], 2011. In: Guide for the Care and Use of Laboratory Animals, eighth ed. Institute for Laboratory Animal Research, Division on Earth and Life Studies. National Academy of Sciences, Washington (DC).
- Nema, R.K., Yadav, S., Mandal, S., Yadav, S., 2009. Antioxidants: a review. *J. Chem. Pharmaceut. Res.* 1 (1), 102–104.
- Newman, D., 2008. Natural products as leads to potential drugs: an old process or the new hope for drug discovery. *J. Med. Chem.* 51, 2589–2599.
- Njoku, U.O., Nwodo, O.F.C., Ougufor, M.O., 2017. Cardioprotective potential of methanol extract of *Costus afer* leaf on carbon tetrachloride-induced cardiotoxicity in albino rats. *Asian J. Pharmaceut. Res. Health Care* 9 (2), 51–58.
- Okokon, J.E., Antia, B.S., Essiet, G.A., Nwudu, L.L., 2007. Evaluation of *in vivo* antiplasmodial activity of ethanolic extract of *Lasianthera africana*. *Res. J. Pharmacol.* 1 (2), 30–33.
- Okokon, J.E., Antia, B.S., Umoh, E.E., 2009. Antiulcerogenic activity of ethanolic leaf extract of *Lasianthera africana*. *Afr. J. Tradit. Complement. Altern. Med.* 6 (2), 150–154.
- Okokon, J.E., Nwafor, P.A., Noah, K.J., 2011. Nephroprotective effect of *Croton zambesicus* root extract against gentamicin-induced kidney injury. *Asian Pac. J. Trop. Med.* 4 (12), 969–972.
- Omotuyi, O.I., Nash, O., Inyang, O.K., Ogidigo, J., Enejoh, O., Okpalefe, O., Hamada, T., 2018. Flavonoid-rich extract of *Chromolaena odorata* modulate circulating GLP-1 in Wistar rats: computational evaluation of TGR5 involvement. *3 Biotech.* 8 (2), 124–132.
- Oufir, M., Seiler, C., Gerodetti, M., Gerber, J., Fürer, K., Mennet-von Eiff, M., Potterat, O., 2015. Quantification of bufadienolides in *Bryophyllum pinnatum* leaves and manufactured products by UHPLC-ESI/MS. *Planta Med.* 81 (12/13), 1190–1197.
- Procházková, D., Boušová, I., Wilhelmová, N., 2011. Antioxidant and pro-oxidant properties of flavonoids. *Fitoterapia* 82 (4), 513–523.
- Rekha, C., Poornima, M., Manasa, M., Abhisha, V., Devi, P.J., Kumar, V.H.T., Kekuda, P.T.R., 2012. Ascorbic acid, total phenol content and antioxidant activity of fresh juices of four ripe and unripe citrus fruits. *Chem. Sci. Trans.* 1 (2), 303–310.
- Shah, M.D., Gnanaraj, C., Haque, A.T.M.E., Iqbal, M., 2015. Antioxidative and chemopreventive effects of *Nephrolepis biserrata* against carbon tetrachloride-induced oxidative stress and hepatic dysfunction in rats. *Pharm. Biol.* 53 (1), 31–39.
- Shodehinde, S.A., Oyeleye, S.I., Adebayo, A.A., Oboh, G., Olasehinde, T.A., Boligon, A.A., 2017. *Lasianthera africana* leaves inhibits  $\alpha$ -amylase  $\alpha$ -glucosidase, angiotensin-1 converting enzyme activities and Fe<sup>2+</sup>-induced oxidative damage in pancreas and kidney homogenates. *Orient. Pharm. Exp. Med.* 17 (1), 41–49.
- Singh, N., Kamath, V., Narasimhamurthy, K., Rajini, P.S., 2008. Protective effects of potato peel extract against carbon tetrachloride-induced liver injury in rats. *Environ. Toxicol. Pharmacol.* 26 (2), 241–246.
- Skeggs, L.T., Hochstrasser, H.C., 1964. Colorimetric method for chloride estimation in serum and plasma. *Clin. Chem.* 10, 918–920.
- Stander, M.A., Van Wyk, B., Taylor, M.J.C., Long, H.S., 2017. Analysis of phenolic compounds in rooibos tea (*Aspalathus linearis*) with a comparison of flavonoid-based compounds in natural populations of plants from different regions. *J. Agric. Food Chem.* 65, 10270–10281.
- Teri, A.E., Sesin, P.G., 1958. Determination of potassium in serum, using sodium tetraphenyl boron. *Am. J. Clin. Pathol.* 29, 86–88.
- Trinder, P., 1951. A rapid method for the determination of sodium in serum. *Analyst* 76, 596–599.
- Tunçdemir, M., Mirzazaf, E.B., Uzun, H., 2018. Renoprotective potential of quercetin in experimental diabetic nephropathy: assessing antiapoptotic and antioxidant effects. *Arch. Clin. Exp. Med.* 3 (3), 179–185.
- Videla, L.A., 2009. Oxidative stress signalling underlying liver disease and hepatoprotective mechanisms. *World J. Hepatol.* 1 (1), 72–78.
- Wang, Y.D., Zhang, Y., Sun, B., Leng, X.W., Li, Y.J., Ren, L.Q., 2017. Cardioprotective effects of rutin in rats exposed to pirarubicin toxicity. *J. Asian Nat. Prod. Res.* 20 (4), 361–373.
- Xu, D., Hu, M.J., Wang, Y.Q., Cui, Y.L., 2019. Antioxidant activities of quercetin and its complexes for medicinal application. *Molecules* 24, 1123–1138.
- Yi, Y., Zhang, Q.W., Li, S.L., Wang, Y., Ye, W.C., Zhao, J., Wang, Y.T., 2012. Simultaneous quantification of major flavonoids in “Bawanghua”, the edible flower of *Hylocereus undatus* using pressurised liquid extraction and high performance liquid chromatography. *Food Chem.* 135 (2), 528–533. In this issue.
- Zhishen, J., Mengcheng, T., Jianming, W., 1999. The determination of flavonoid contents in mulberry and their scavenging effects on superoxide radicals. *Food Chem.* 64 (4), 555–559.
- Zhou, C., Luo, Y., Lei, Z., Wei, G., 2018. UHPLC-ESI-MS analysis of purified flavonoids fraction from stem of *Dendrobium denneanum* Paxt. and its preliminary study in Inducing apoptosis of HepG2 cells. *Evid-Based. Compl. Alt. Med.*, 8936307